

# High-Resolution Characterization of the Region Around Manganese Sulfide Inclusions in Stainless Steel Alloys

Q. Meng,\* G.S. Frankel,†\*\* H.O. Colijn,\* and S.H. Goss\*\*

## ABSTRACT

*The region between manganese sulfide (MnS) inclusions and the matrix in several stainless steels (SS) was carefully characterized using high-resolution scanning transmission electron microscopy (STEM) line profiling in combination with focused ion beam (FIB) sectioning and secondary ion mass spectrometry (SIMS) mapping. In contradiction to the recent findings of Ryan, et al., no Cr depletion zone around MnS inclusions was found in the SS, including the exact Type 316F (UNS S31620) SS sample used in their study.*

**KEY WORDS:** inclusions, sensitization, stainless steels

## INTRODUCTION

Ryan, et al.,<sup>1</sup> recently have published results that present a new explanation for the deleterious effects of sulfides on the localized corrosion resistance of stainless steels (SS). It was suggested that this new view will allow improvement of corrosion properties by “unconventional heat treatments” and that “basic grades of SS could find wider application” as a re-

sult.<sup>2</sup> A rather wide zone (about 0.5  $\mu\text{m}$ ) depleted in Cr was found around manganese sulfide (MnS) inclusions in a Type 316F (UNS S31620)<sup>(1)</sup> grade SS using secondary ion mass spectrometry (SIMS) analysis of areas selectively sputtered by a focused ion beam.<sup>1</sup> Such depleted zones were predicted in an earlier work by Williams and Zhu in which artificial inclusions were given high-temperature treatments.<sup>3</sup> According to this view, the MnS inclusions solidify at lower temperatures than the SS matrix and, in the molten state, will dissolve Cr from the neighboring lattice region. It was suggested that pitting is triggered by dissolution of the Cr depletion zone, which then activates the sulfide inclusions. However, it is commonly accepted<sup>4-6</sup> that pits in SS are initiated by either chemical or electrochemical dissolution of the sulfides to form an aggressive species that accelerates local attack. An investigation was undertaken to confirm the findings of Ryan, et al., using different techniques. A brief communication on this work has been published recently;<sup>7</sup> this paper will provide the details. Several different materials were investigated, including a commercial grade of Type 304 (UNS S30400) SS, Type 316F SS in the as-cast and annealed conditions, and the same piece of Type 316F used in the study by Ryan, et al. In contradiction to the findings of Ryan, et al.,<sup>1</sup> no evidence of Cr-depleted zones was found in any of the materials studied, including the same Type 316F material that they used in their study.

Submitted for publication May 2003; in revised form, September 2003.

† Corresponding author. E-mail: frankel.10@osu.edu.

\* Fontana Corrosion Center, Department of Materials Science and Engineering, The Ohio State University, Columbus, OH 43210.

\*\* Department of Electrical Engineering, The Ohio State University, Columbus, OH 43210.

<sup>(1)</sup> UNS numbers are listed in *Metals and Alloys in the Unified Numbering System*, published by the Society of Automotive Engineers (SAE International) and cosponsored by ASTM International.

**TABLE 1**  
Compositions of SS Alloys (wt%)

	Cr	Ni	Mo	Mn	S	Si	C	Fe
Type 304 <sup>(A)</sup>	19	9.25	—	2.0	0.03	1.0	0.08	Bal.
As-cast Type 316F	17.3	11.98	2.61	1.72	0.14	0.55	0.015	Bal.
RWCHM <sup>(B)</sup>	17.65	8.61	2.19	0.67	0.16	0.51	0.062	Bal.

<sup>(A)</sup> The composition of Type 304 is nominal and not measured.

<sup>(B)</sup> The composition of Type 316F used by Ryan, et al., was reported in their paper.<sup>1</sup>

## EXPERIMENTAL PROCEDURES

### Materials

Several different SS alloys were studied in this work including a commercial-grade Type 304, Type 316F in the as-cast and annealed conditions, and the same piece of Type 316F used in the study by Ryan, et al.<sup>1</sup> The latter material will be referred to as the RWCHM sample. The compositions of the SS alloys are listed in Table 1. The as-cast Type 316F is a pellet that was extracted from a large melt for analysis purposes. Part of the as-cast Type 316F pellet was annealed at 1,100°C for 1 h and quenched in water at room temperature. All sample surfaces were polished using a nonaqueous polishing procedure to limit corrosion during polishing. The samples were mechanically ground with successively finer silicon carbide (SiC) paper through 1200 grit, then polished down to 0.05  $\mu\text{m}$  with a suspension of alumina in ethanol, and finally cleaned ultrasonically with ethanol.

### Transmission Electron Microscopy

#### Sample Preparation

Cross sections through MnS inclusions were prepared with an FEI Strata Dual Beam 235<sup>†</sup> focused ion beam (FIB) tool using a 30-keV Ga<sup>+</sup> ion beam and a 5-keV electron beam. The membranes had areas of 15  $\mu\text{m}$  by 5  $\mu\text{m}$ , and were thinned in the FIB to a thickness of <200 nm for electron transparency. The membrane was plucked under an optical microscope using a sharp borosilicate glass needle of about 1  $\mu\text{m}$  diameter, and placed on a 200 mesh Au specimen grid with a formvar/carbon support film for transmission electron microscopy/scanning transmission electron microscopy (TEM/STEM) analysis.

### STEM and Nano-Energy-Dispersive Spectroscopy Profiling

Energy-dispersive spectroscopy (EDS) line profiles were acquired using an FEI Tecnai TF20<sup>†</sup> STEM operating at 200 kV. The electron probe size is <2 nm and the step size is about 10 nm. The collection time per point is 5 s. The drift-corrected EDS line profiles

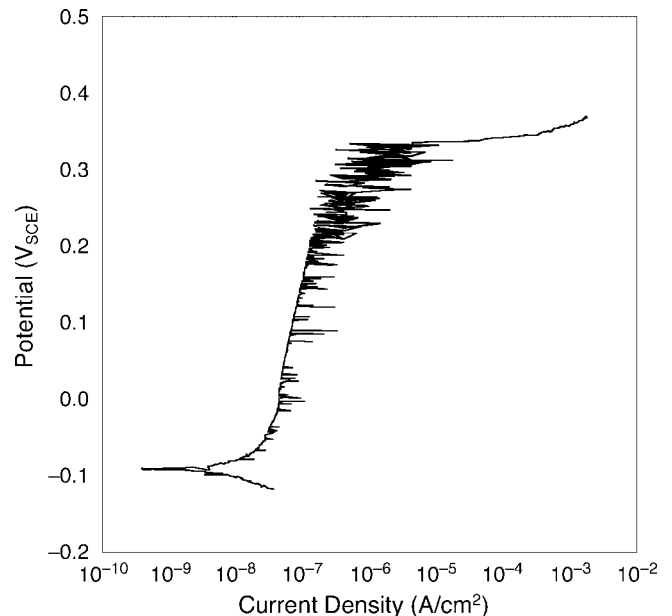


**FIGURE 1.** Potentiodynamic polarization curve for Type 304 in aerated 0.5 M NaCl.

were acquired and quantified using the FEI/Emispec TIA<sup>†</sup> software. The EDS quantification used the Cliff-Lorimer method with theoretical k-factors.

### SIMS Analysis

Element mapping was performed on MnS inclusions in different pieces taken from the Type 304 and Type 316F used by Ryan, et al., using a Physical Electronics<sup>†</sup> time-of-flight secondary ion mass spectrometry (SIMS) with a Ga<sup>+</sup> ion analysis source. Before mapping, the sample was sputtered with a 1-kV Cs<sup>+</sup> ion beam to remove surface organic contaminants. Secondary electron imaging was used first to locate MnS inclusions. Then the positive and negative ion modes were used to map positive and negative ions separately. The spot size of the Ga<sup>+</sup> ion beam was about 150 nm and the Ga<sup>+</sup> ion current was 600 pA. The time for each image was 2 min.

### Electrochemical Test

Potentiodynamic polarization experiments were performed on samples of the Type 304 stock in aerated 0.5 M NaCl. The sample was ground to 1200 grit

<sup>†</sup> Trade name.

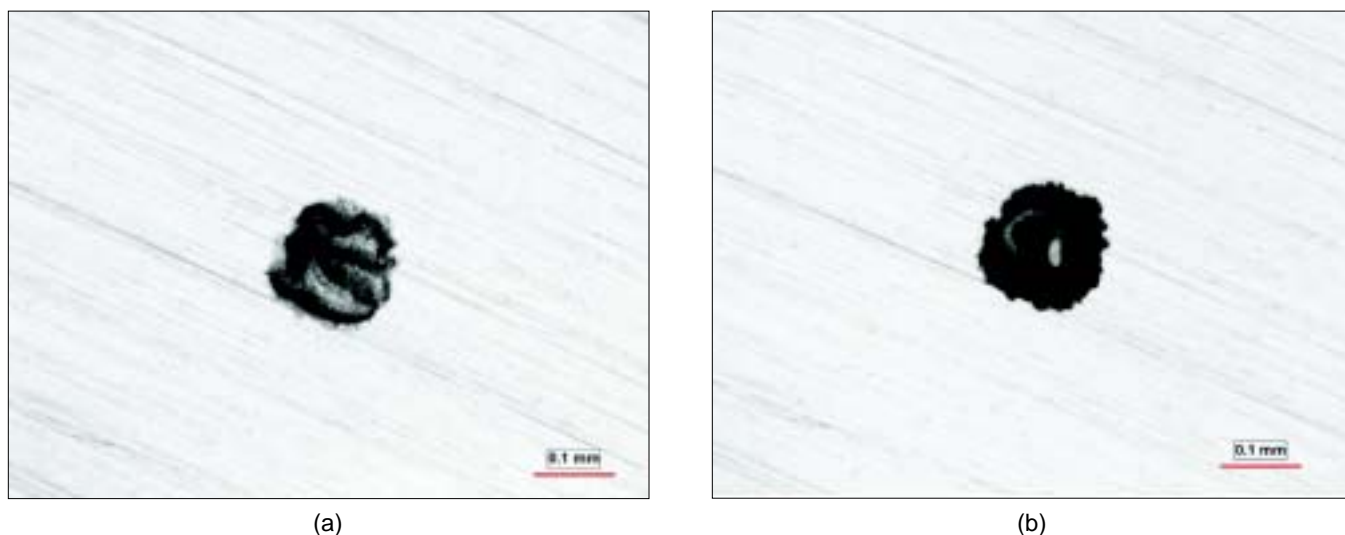


**FIGURE 2.** Optical micrographs of a pit observed after the polarization: (a) before and (b) after ultrasonic cleaning in deionized water.

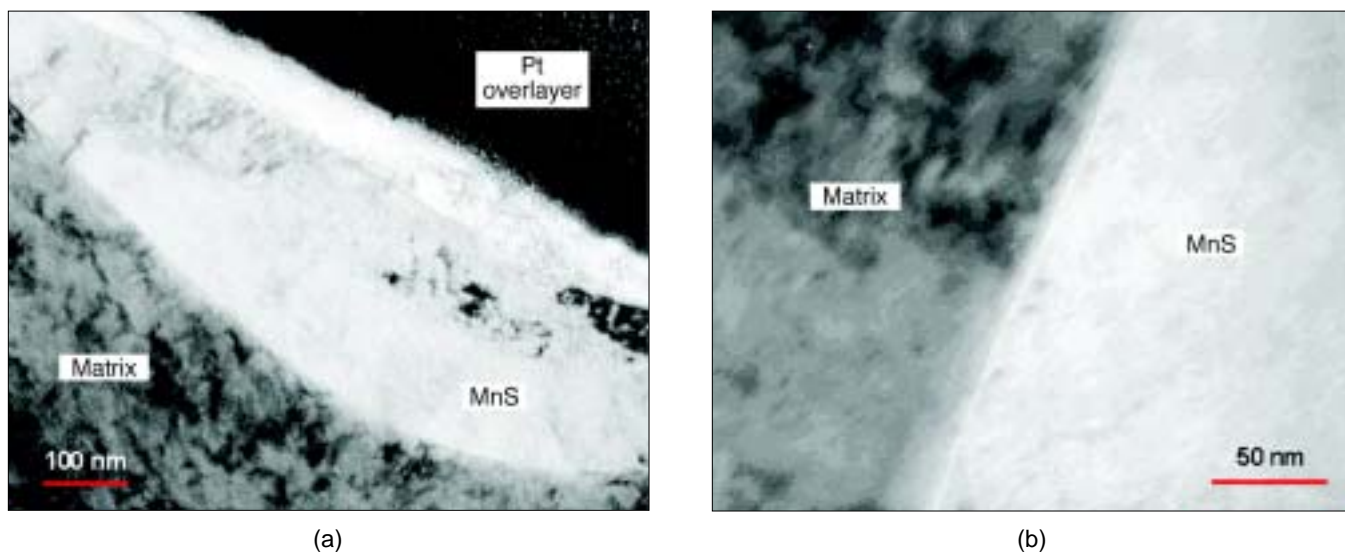


**FIGURE 3.** Bright-field TEM micrographs of (a) MnS inclusion and (b) the sharp interface of MnS inclusion and adjacent matrix in Type 304.

and masked with black wax. A saturated calomel reference electrode (SCE) and a Pt mesh counter electrode were used. The scan rate was 0.2 mV/s. After polarization, the corrosion morphology of the sample was examined with an optical microscope.

## RESULTS

### Commercial-Grade Type 304

If Cr-depleted zones around sulfide inclusions are generally responsible for pitting corrosion in SS, such zones should be evident in a sample taken from a commercial grade of standard Type 304 SS. Figure 1 shows a typical anodic polarization curve for this Type 304 SS in aerated 0.5 M NaCl. Many current

transients associated with metastable pits are evident throughout the passive region, and stable breakdown was found at 330 mV<sub>SCE</sub>. This is a typical value for Type 304 SS. Microscopic observation following the experiment indicated the presence of some crevice attack beneath the black wax and pits in the matrix of the steel distant from the crevice. Figure 2 shows the morphology of a typical pit after polarization. These results indicate that this Type 304 material is indeed susceptible to pitting corrosion, as expected.

Two different approaches were used to determine if Cr-depleted zones were associated with MnS inclusions in this Type 304 SS, and therefore might be the cause of the pitting susceptibility. STEM line profil-

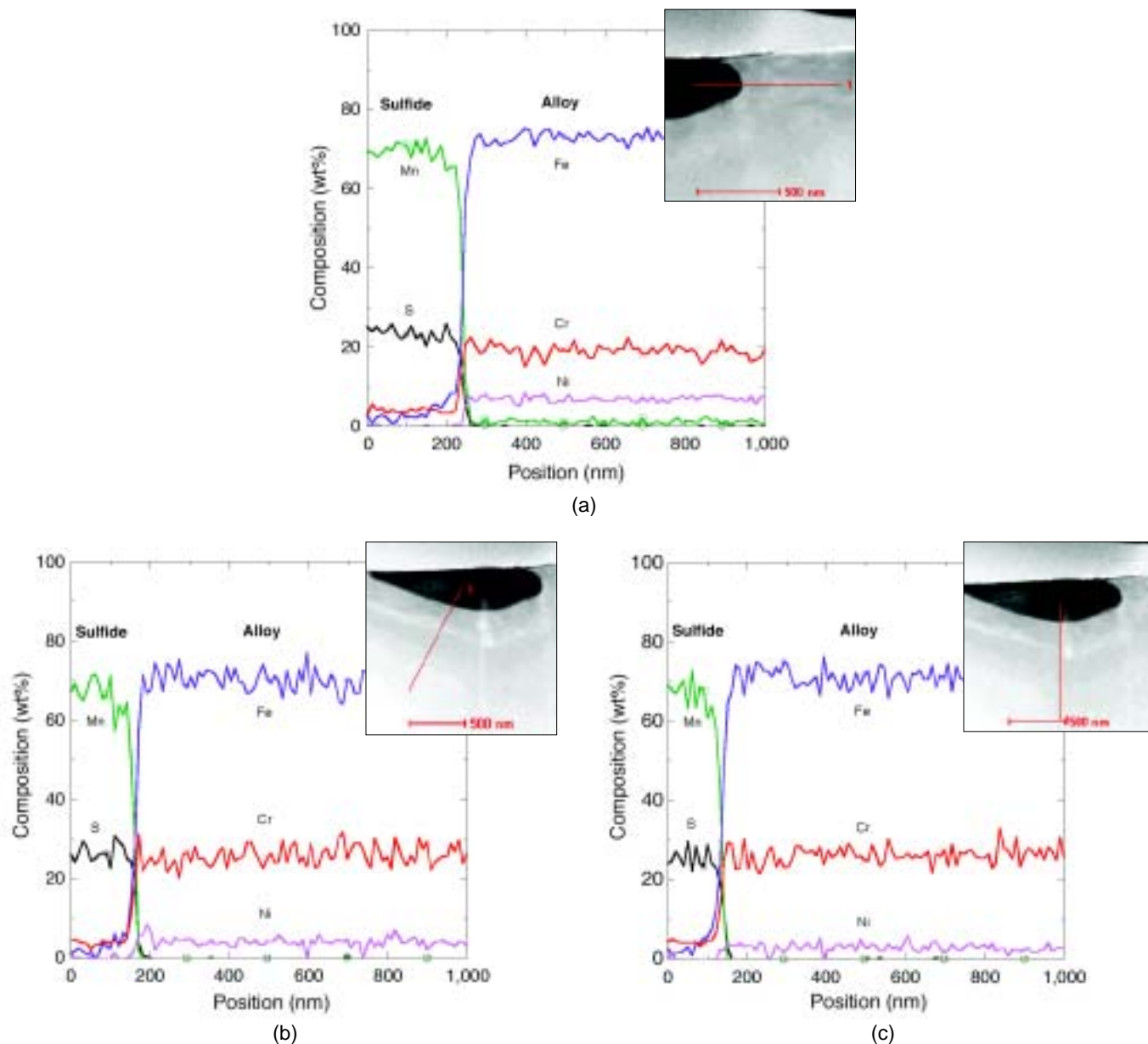


**FIGURE 4.** Composition profiles across the interface of MnS inclusion and adjacent matrix in Type 304 in the (a) horizontal, (b) vertical, and (c) diagonal directions. The inset micrographs show the lines along which the analyses were made. The dark spot in the images is the MnS particle, and the bright area on the top is the protective Pt layer.

ing analysis has superior lateral resolution and SIMS mapping has excellent sensitivity.

Figure 3(a) is a bright-field TEM micrograph of a cross section on an MnS inclusion from the Type 304 SS. A Pt protective layer was deposited on the MnS inclusion in the FIB chamber prior to FIB cross-sectioning. STEM mapping indicated that a layer of manganese oxide existed between the Pt layer and the MnS particle. This oxide layer is a corrosion product formed on the MnS inclusion as a result of the polishing process and ambient atmosphere exposure. The higher magnification TEM micrograph shown in Figure 3(b) reveals that the interface of

MnS inclusion and adjacent matrix was sharp and clear.

STEM line profiling was performed across the MnS/matrix interface in horizontal, diagonal, and vertical directions (Figure 4). The probe size was <math><2\text{ nm}</math> with a step size of 10 nm. During collection of the x-ray signal, correction was made for sample drift, ensuring that the profile was made exactly along the lines drawn on the inset TEM images. The data in these figures are noisy due to the short dwell time per data point, but this is compensated for by the large number of data points. This noise or scatter came originally from counting statistics used in EDS

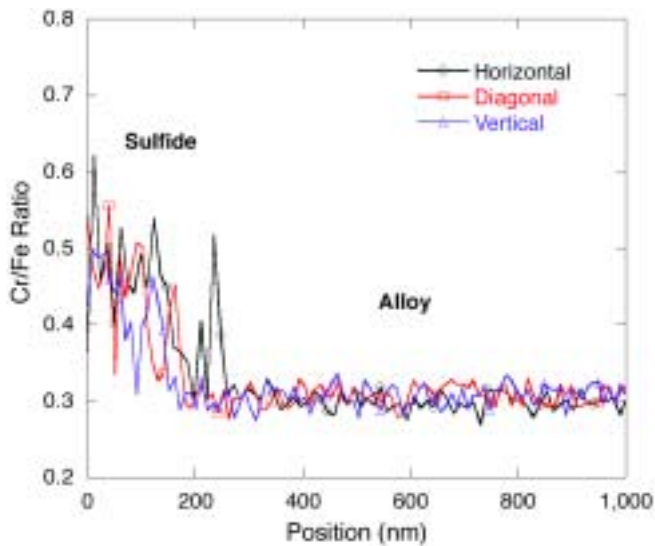


**FIGURE 5.** Ratio of Cr/Fe signals from raw EDS data for linescans in three directions shown in Figure 4.

acquisition. It is further magnified by the conversion of the data to concentration. To reduce the scatter in concentration profiles, raw integrated intensities of Cr and Fe signals were extracted and intensity ratios

of Cr to Fe were calculated. Figure 5 shows the Cr/Fe intensity ratios for the three scans in Figure 4. This form of the data is analogous to the form of Figure 1 in the paper by Ryan, et al.,<sup>1</sup> except that the ratio is not further normalized to unity in the matrix, as was done by Ryan, et al. The Cr/Fe ratios are higher in the sulfide inclusion than in the matrix region, which are equal to 0.3 with little scatter for the three scans. Constant Cr/Fe intensity ratio indicates that Cr/Fe concentration ratio in the matrix is constant since there is a proportional relationship between x-ray intensity and concentration in the Cliff-Lorimer method. No trend of a decrease in the Cr/Fe ratio near the inclusion is evident in Figure 5. The line profiles shown in Figure 4 also reveal a compositionally sharp interface of the MnS inclusion and matrix, which indicates that there was no Cr depletion zone around the MnS inclusion in commercial-grade Type 304 SS.

SIMS mapping was performed on a different MnS inclusion with focused Ga ion analysis beam as shown in Figure 6. The lateral resolution of the SIMS mapping was about 150 nm. Several 10- $\mu\text{m}$  by 10- $\mu\text{m}$  regions were mapped using both positive and negative modes to detect positive and negative secondary ions, respectively. There was a slight position

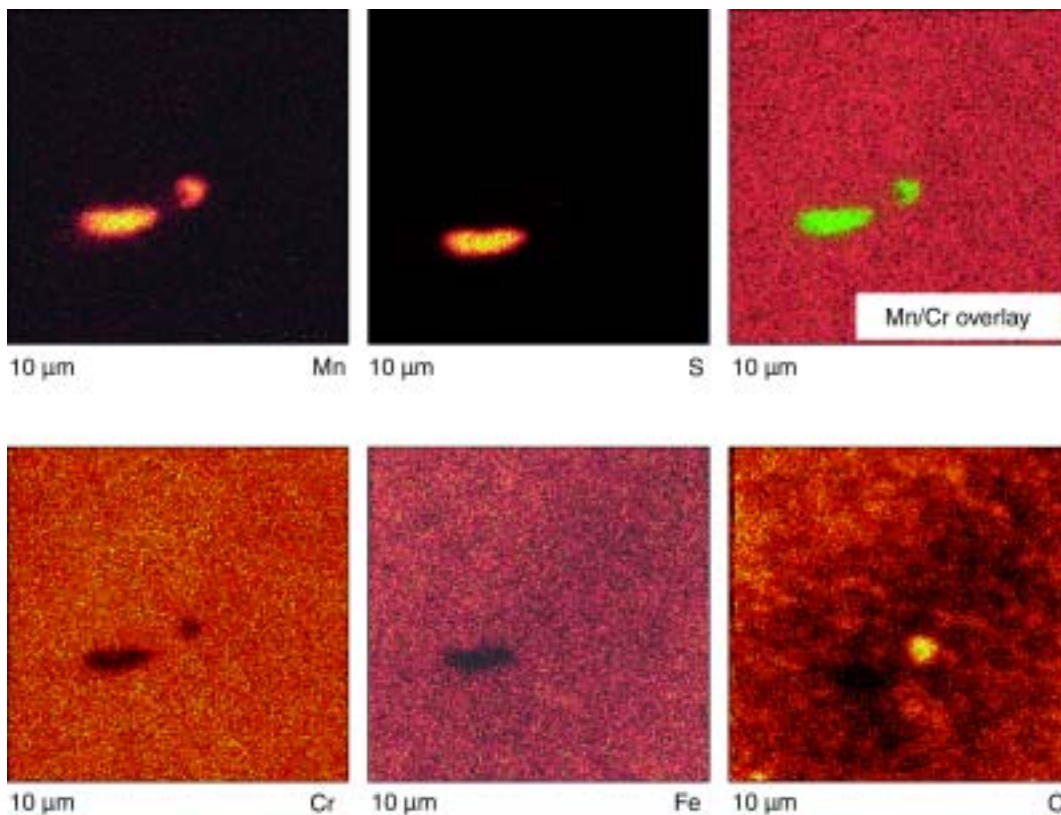


**FIGURE 6.** SIMS mapping of MnS inclusion in Type 304, 10- $\mu\text{m}$  by 10- $\mu\text{m}$  mapping area. Mn/Cr overlay where Mn is green and Cr is red evidencing no Cr depletion region in the matrix around MnS inclusion. The round particle near MnS inclusion is manganese oxide.

shift when switching polarity. In Figure 6, elemental Mn and S maps reveal one MnS particle about 1  $\mu\text{m}$  in size, which corresponds to the shadows in the Cr and Fe maps. The overlay of Mn and Cr maps, where Mn is green and Cr is red, reveals that the MnS particle exactly matched the Cr shadow. In addition, one round manganese oxide particle was observed near the MnS particle, as evidenced by the Mn and O maps. These observations further indicate no Cr depletion zone around MnS inclusions in Type 304 SS.

#### *As-Cast and Annealed Type 316F*

The Type 316F SS is a free machining grade with extremely high sulfur content, which counteracts the beneficial influence of the high Cr and Mo content added for good corrosion resistance, and is not widely used. To check if the observations of Ryan, et al., were specific to this grade of SS, Type 316F also was studied. The Type 316F sample was originally in the as-cast condition, being a sample that was vacuum-extracted from a melt for chemical analysis. Part of the as-cast Type 316F sample was annealed at 1,100°C for 1 h and quenched in water. The as-cast and annealed structures should provide ample opportunity for Cr segregation to the sulfides and depletion in the matrix, as described by Williams and Zhu.<sup>3</sup>

Figure 7 shows bright-field TEM micrographs of cross sections of two MnS inclusions (labeled A and B) in the as-cast Type 316F SS. These inclusions were in the interdendritic region of the cast microstructure, and the matrix surrounding the inclusions was multiphase. STEM analysis revealed that the interdendritic region was rich in Mo and Nb.

Figures 8 and 9 show EDS line profiling across the MnS inclusions A and B, respectively. The conditions were the same as were described above for Type 304 SS. The profiling was made along the lines drawn on the inset TEM micrographs in Figures 8 and 9. Inclusion A was embedded in the interdendritic region rich in Mo and Nb. Except for a small region, inclusion B was surrounded by the SS matrix. The line profiles into the interdendritic region or into the steel matrix both indicate no Cr-depleted zone in as-cast Type 316F.

Figure 10(a) is a dark-field TEM image of the Type 316F sample annealed at 1,100°C for 1 h and quenched in water at room temperature. The interdendritic region found in the as-cast Type 316F was not evident after annealing. EDS line profiling was made along the line drawn on the TEM micrograph shown in Figure 10(a). The compositional line profiles, as shown in Figure 10(b), clearly indicate that the interface between sulfide and matrix is compositionally sharp. Therefore, it is evident that no Cr depletion zone exists in the region around MnS inclusion in annealed Type 316F.

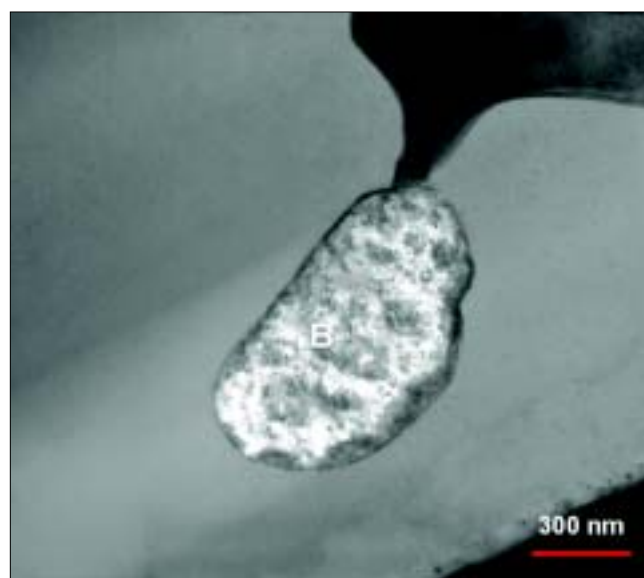
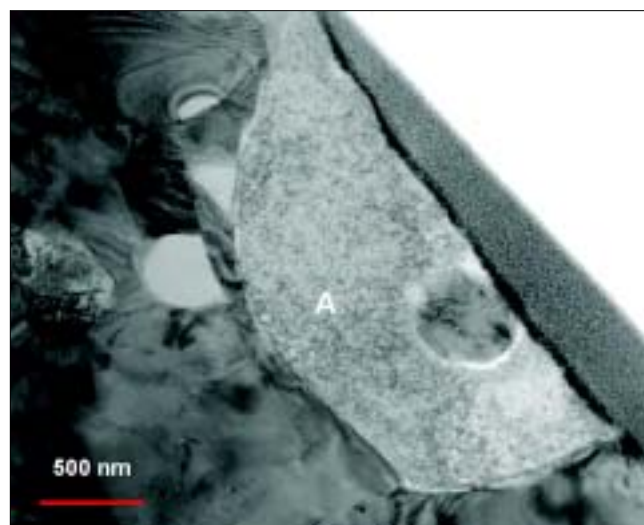
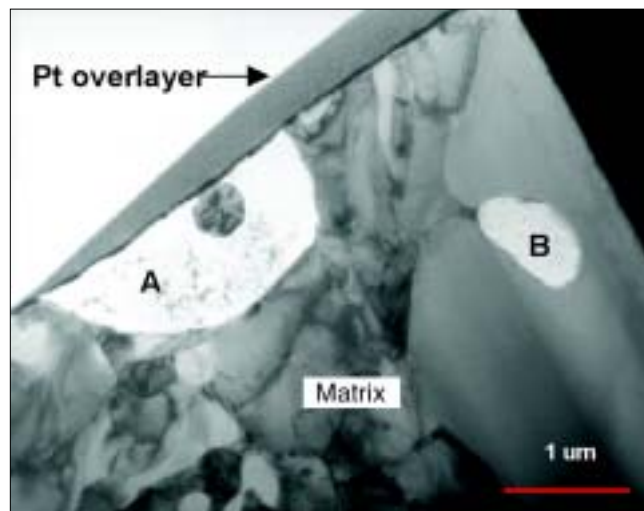


**FIGURE 7.** Bright-field TEM micrographs of MnS inclusions in as-cast Type 316F.

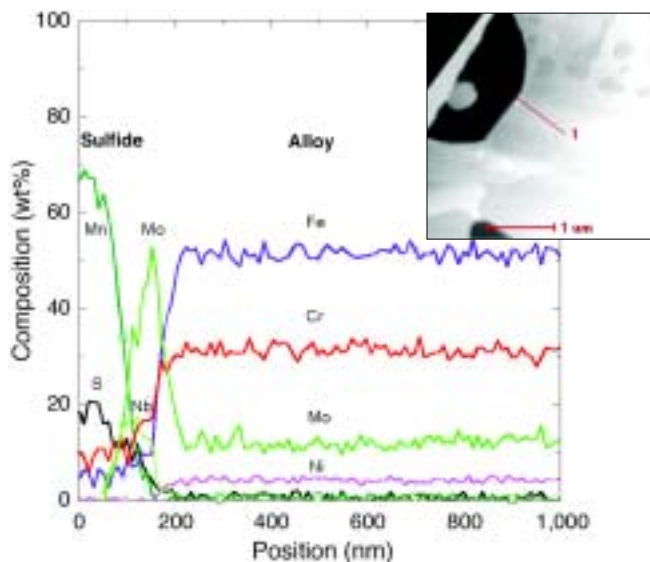


FIGURE 8. Composition profile across the interface of MnS inclusion A and adjacent matrix in as-cast Type 316F.

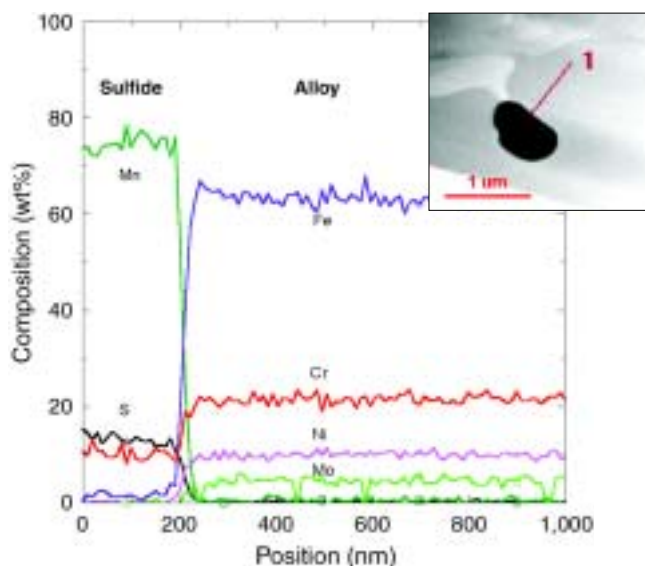
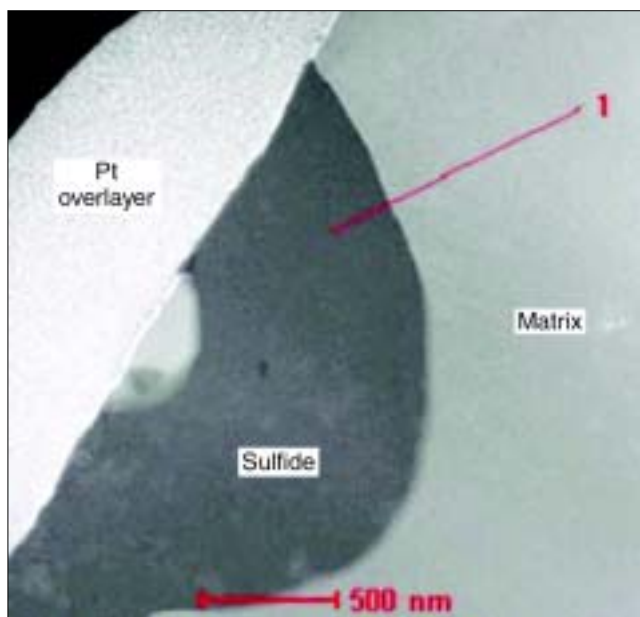
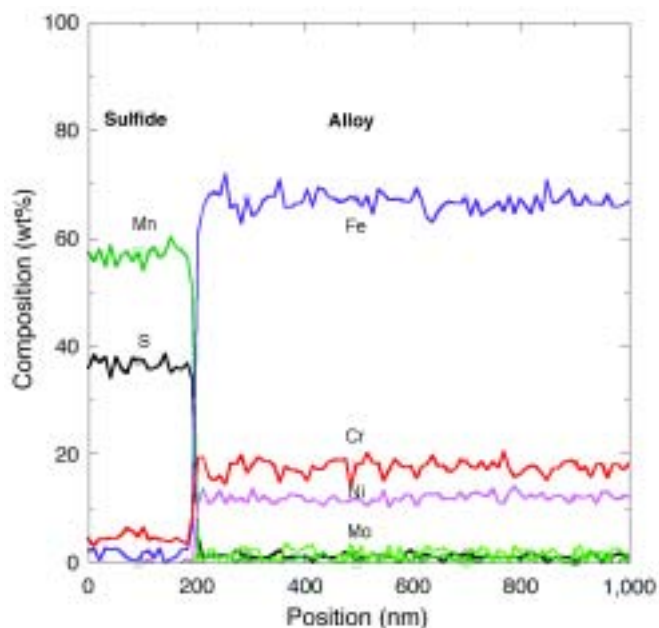


FIGURE 9. Composition profile across the interface of MnS inclusion B and adjacent matrix in as-cast Type 316F.



(a)



(b)

FIGURE 10. (a) Dark-field TEM image of sulfide particle and (b) composition profile across the interface of MnS inclusion and adjacent matrix in annealed Type 316F sample.

### RWCHM Sample

As described above, no Cr depletion zone exists in the commercial-grade Type 304 and Type 316F in the as-cast and annealed conditions. SIMS mapping and STEM line profiling was performed to investigate the same piece of Type 316F used in the study by Ryan, et al.<sup>1</sup> Figure 11 shows SIMS mapping of a 20- $\mu\text{m}$  by 20- $\mu\text{m}$  region containing four inclusions: three MnS and one manganese oxide. For the MnS

inclusions, elemental Mn and S maps reveal MnS particles about 2  $\mu\text{m}$  in size, which match the corresponding shadows in Cr and Fe maps. This SIMS result is in good agreement with those for Type 304 SS. No Cr depletion in the RWCHM Type 316F sample is evident in SIMS mapping.

Figure 12(a) shows a dark-field TEM image of a sulfide inclusion in the RWCHM sample. In this Type 316F sample, a majority of the sulfide inclu-

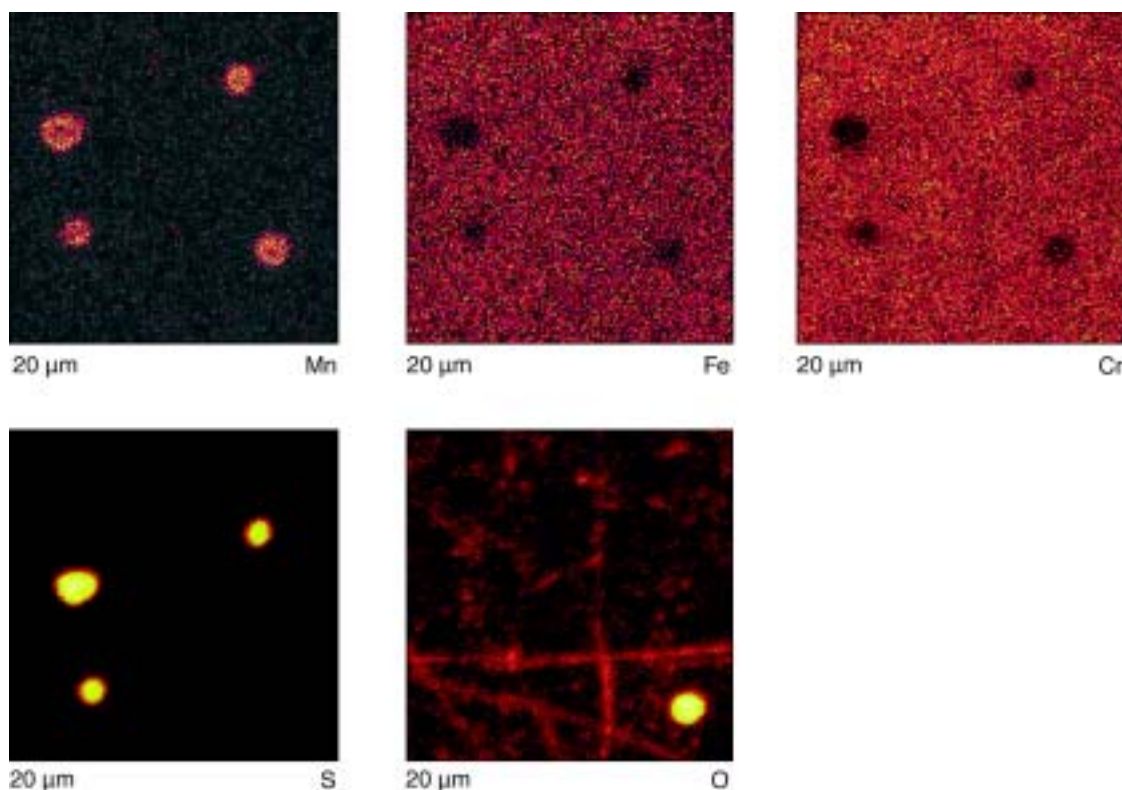


**FIGURE 11.** SIMS mapping of MnS inclusions in RWCHM sample,<sup>1</sup> 20- $\mu$ m by 20- $\mu$ m mapping area. Three MnS and one MnO inclusions were found in this mapping area.

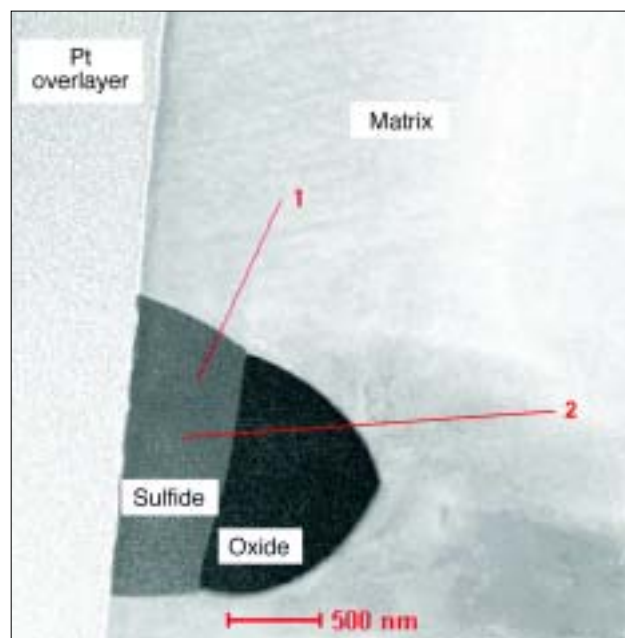
sions are connected to oxides, and the darker part of the inclusion is the oxide phase. EDS linescans for several elements are shown in Figure 12(b) for a scan along the line labeled 1 in Figure 12(a). This line crosses the boundary between the MnS inclusion and matrix. The linescans shown in Figure 12(b) are identical to the results of analyses performed on sulfide inclusions from the other SS described above. There is a sharp change in composition at the interface of the MnS inclusion and matrix with no evidence of a Cr depletion zone around the MnS inclusion.

Figure 12(c) shows the results of a scan made along the line labeled 2 in Figure 12(a), from the sulfide, through the oxide, and then into the matrix. The Cr concentration is lower in the oxide than in the matrix, and even lower in the sulfide. The resulting Cr profile appears to have a Cr-depleted region, but this is really the effect of the oxide particle. It should be noted that the Fe content in the oxide decreases more than the Cr content relative to the bulk concentration, resulting in a higher Cr/Fe concentration ratio in the oxide. SIMS measurements at these particles found that the (mass 52)/(mass 56) Cr/Fe ion yield ratio was similar or slightly higher in the oxides relative to the matrix. Therefore, the depleted zone reported by Ryan, et al., cannot be rationalized by the effects of oxides adjoining the sulfide particles.

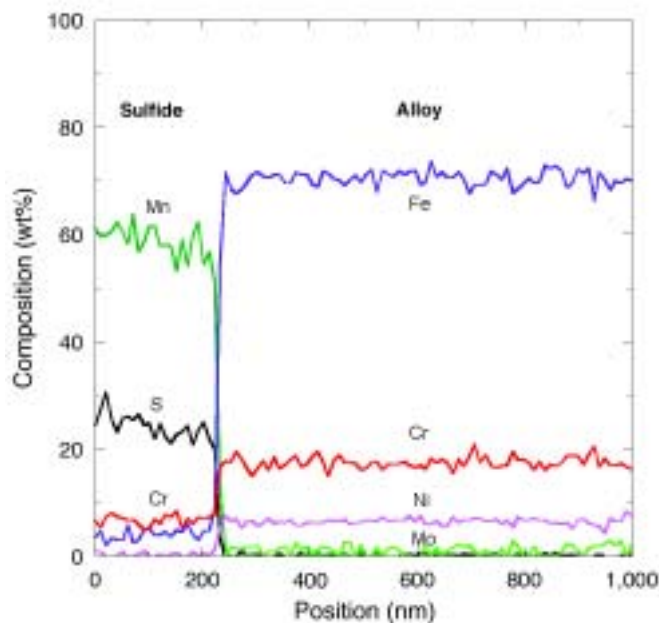
Figure 13 shows the ratio of the raw EDS data for the linescan from the sulfide to the matrix in Figure 12(b), with the ratio normalized to unity in the matrix. This curve is perfectly analogous to the SIMS data shown in Figure 1(a) in the paper by Ryan, et al.<sup>1</sup> Figure 13 exhibits little scatter and no evidence of a depleted zone near the sulfide. There is a sharp transition to the higher Cr/Fe ratio inside the sulfide particle.

## DISCUSSION

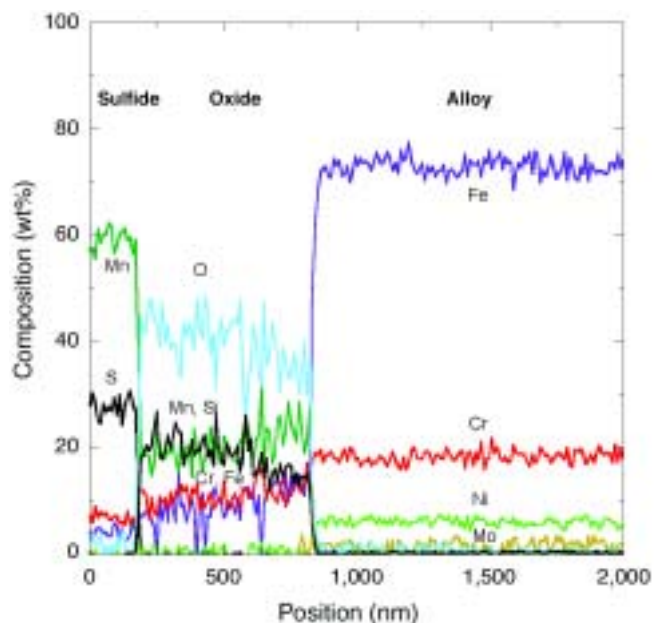
Henthorne<sup>8</sup> studied the effect of Mn content on the sulfide composition and corrosion resistance of resulfurized free-machining SS. Using electron microprobe analysis, he found that the Cr content in the sulfides increased as the nominal Mn content in the steel decreased. Furthermore, the corrosion rate decreased as the steel Mn content decreased for exposure to a wide range of environments, including acids, salt spray, and high humidity. As shown in Table 1, the RWCHM sample and the as-cast Type 316F sample have vastly different Mn contents, which might affect the interaction between the Cr in the alloy and the sulfide. However, our findings indicate that MnS inclusions in neither alloy exhibited Cr depletion zones, so alloy Mn content is not critical to the formation of these zones.



(a)



(b)



(c)

**FIGURE 12.** (a) Dark-field TEM image of a typical mixed sulfide/oxide particle in the Type 316F sample used in the RWCHM sample.<sup>1</sup> The darker region is the oxide. The lines labeled 1 and 2 indicate the locations of the EDS scans shown in (b) and (c), respectively.

In a recent response to the findings of this study,<sup>9</sup> Ryan and Williams indicated that only about 20% of the 25 inclusions they studied from the Type 316F sample exhibited a Cr depletion region and about 20% exhibited no depletion. The data from the rest were complicated by sputtering of the inclusion itself. They suggest that this variation in behavior might explain why all MnS inclusions do not generate pits. In the course of this study, 17 in-

clusions from three alloy sources were investigated by STEM and SIMS, and no evidence of Cr depletion was found. Additional work is required to prove if this is only a statistical anomaly. Finally, it is possible that heat treatments other than those studied in this work (as-cast, annealed at 1,100°C for 1 h, and as-received commercial plate) would be more likely to result in Cr-depleted zones near sulfide inclusions.

## CONCLUSIONS

❖ High-resolution STEM profiling on cross sections of MnS particles and SIMS mapping on the surface provided no evidence that Cr depletion zones exist around MnS inclusions in the SS studied, at least within a region on the order of nm in size. This is in contradiction to the results of Ryan, et al.<sup>1</sup>

## ACKNOWLEDGMENTS

The authors acknowledge D.E. Williams for providing the Type 316F sample he used in the previous study, and T. Wood of Electralloy for providing the cast Type 316F sample. Collegial interaction with M.P. Ryan and D.E. Williams over the data interpretation also is greatly appreciated.

## REFERENCES

1. M.P. Ryan, D.E. Williams, R.J. Chater, B.M. Hutton, D.S. McPhail, *Nature* 415 (2002): p. 770.
2. R.C. Newman, *Nature (News and Views)* 415 (2002): p. 743.
3. D.E. Williams, Y.Y. Zhu, *J. Electrochem. Soc.* 147 (2000): p. 1,763.
4. A.J. Sedriks, *Corrosion of Stainless Steels* (New York, NY: Wiley-Interscience, 1996), p. 126.
5. G.S. Frankel, *J. Electrochem. Soc.* 145 (1998): p. 2,186.
6. R.C. Newman, H.S. Isaacs, B. Alman, *Corrosion* 38 (1982): p. 261.
7. Q. Meng, G.S. Frankel, H.O. Colijn, S.H. Goss, *Nature* 424 (2003): p. 389.
8. M. Henthorne, *Corrosion* 26 (1970): p. 511.
9. M.P. Ryan, D.E. Williams, *Nature* 424 (2003): p. 390.

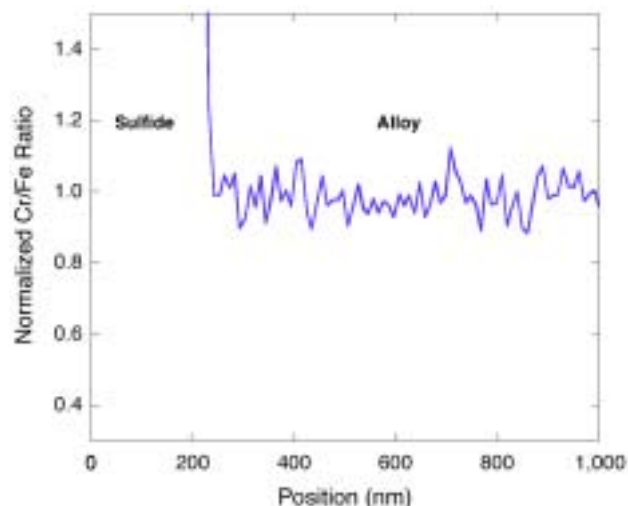


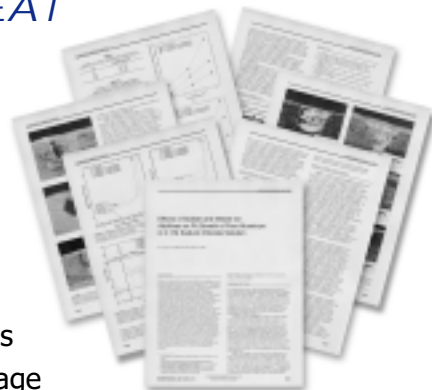
**FIGURE 13.** Ratio of Cr/Fe signals from raw EDS data for the linescan shown in Figure 12(b). The ratio has been further normalized to unity to match the form of Figure 1(a) in the paper by Ryan, et al.<sup>1</sup>

Need  
reprints  
of  
*CORROSION*  
ads,  
articles,  
or  
covers?

THE JOURNAL OF SCIENCE AND ENGINEERING  
**CORROSION**

## REPRINTS ARE A GREAT INVESTMENT!

- ❖ Increase your company's exposure at trade shows and conferences
- ❖ Promote your company's products and services
- ❖ Generate sales through direct mail campaigns and sales calls
- ❖ Promote your professional image as an industry expert
- ❖ Educate employees and colleagues on the latest industry trends and technology
- ❖ And much more!



Professionally printed reprints and photocopied reprints are available of all *CORROSION* ads, articles, and covers. Reprints can be customized with your company's logo, additional product information, or the magazine cover—with no limits on creativity!

Order your reprints today, it simply makes good business sense!  
For reprint information and rates, call 281/228-6219.